Mine Water and the Environment (2022) 41:93–102
https://doi.org/10.1007/s10230-021-00795-x

TECHNICAL ARTICLE

Hydrogeological Effects of Fault Geometry for Analysing Groundwater Inflow in a Coal Mine

Dandan Wang[1] · **Wanghua Sui**[1]

Received: 4 February 2020 / Accepted: 20 July 2021 / Published online: 21 August 2021

Abstract

We investigated the relationship between mine water inflow and fault development. Statistical methods and grey relational analysis (GRA) were used to analyse the relationship between fault complexity and mine water inflow. Major characteristics, such as the fault number, fault strike length, fault throw, fault intersections, and endpoints, were considered to depict fault complexity. The degree of fault complexity was described using a fault influence factor (*E*) and fault fractal dimensions (*D*s). In addition, an inverse distance-weighting interpolation method was used to better describe the fault characteristics. The fault complexity in the study area was divided into four qualitative levels: simple, moderate, relatively complex, and complex. The results show that water pressure and fault complexity have separate nonlinear relationships with mine water inflow. An equation that presents the correlation between parameters and water inflow was derived using the GRA method.

Keywords Water inflow · Fault influence factor · Fault complexity degree · Fault fractal dimension

Introduction

Geo-structural development and groundwater distribution substantially affect the safety of underground construction and mining. Faults and fractures should be carefully investigated because they play a controlling role in groundwater flow and water disasters. Statistically, more than 80% of mine water inrush accidents are related to faults (Wu et al. 2008). Furthermore, fault intersections significantly affect geological structural complexity and their relationship with fluids has been a subject for various studies (Caine and Forster 1999; Dimmen et al. 2017; Eichhubl et al. 2000; Jolley et al. 2007). Fault intersections are also important sites for leakage (Gartrell et al. 2004). In fractured reservoirs, the host rock (i.e. limestone and chalk) generally has less permeability than the faults and fractures that transect them. Fluid flow in such conditions incorporates the effects of pervasive fracture systems, including joints and faults (Jolley et al. 2007). The nature of the fracture system is critical to limestone water abundance.

Considerable work has been done to investigate the correlation between water disasters and what influences them. Li and Yang (1975) analysed the water-rich areas and water abundance of fracture structures with different mechanical properties and found that groundwater recharge and movement were controlled by multiple factors. Niwa et al. (2011) investigated the influence of fault characteristics on groundwater flow, such as fault trace, and the number and width of faults. Meng et al. (2012) classified the fissures that developed in a mine area with the maximum principal curvature method and evaluated the risk of groundwater inrush from the floor. Wu et al. (2014) concluded that groundwater abundance is determined by a variety of factors including aquifer thickness, the specific capacity of water yield, hydraulic conductivity, and geological structures. Zhang et al. (2014) built a numerical model to simulate groundwater outburst from faults. Kang et al. (2018) analysed the characteristics of fault development and proposed a support system for coal mine tunnels.

As mining depth increases, the threat coming from floor-confined limestone water also increases. Fault development and karstification in deep coal mines must be investigated sufficiently to efficiently prevent water disasters. Karst water

✉ Wanghua Sui
suiwanghua@cumt.edu.cn

Dandan Wang
wangdandan@cumt.edu.cn

[1] School of Resources and Geosciences, Institute of Mine Water Hazards Prevention and Controlling Technology, China University of Mining and Technology, Xuzhou 221116, China

inrush is one of the major disasters threatening the coal mining safety in north China. Fang and Fu (2011) analysed the influence of karst water on coal mining from different perspectives using the AHP method, based on a large amount of data from a coal mine in north China. Xu et al. (2012) analysed the features that activate faults and water inflow. Liu et al. (2017) investigated water inrush problems caused by a karst collapse column. The structure, especially fault and fissure development in a coal mining area, plays an important role in mine safety because well-developed, water-conducting faults and fissures could cause the water flow into panels and then cause hazards (Shi and Singh 2001; Wu et al. 2004). It has been widely verified that an area with a strong fracture system is more likely to have a water inrush disaster.

Statistical methods are commonly used to solve fracture problems based on fault geometry characteristics, such as the number of faults, fault strike length, fault throw, and fault intersections. In addition to geological structural complexity, the influential factors, area precipitation, water inrush location, and water inflow should also be analysed (Li et al. 2011; Liang et al. 2015). The fractal dimension can be effectively used to analyse the fault trace (Bagde et al. 2002; Charkaluk et al. 1998; Liu et al. 2015; Mandelbrot and Wheeler 1982). Of these, box-counting is one of the most widely used methods and was used in this study (Ai et al. 2014).

Previous studies have mainly focused on the characteristics of structure development, rather than on the relationship between the quantitative complexity of fault development and groundwater abundance of aquifers. We used the fault influence factor (E) and fractal dimension (Ds) to quantitatively describe the fault characteristics and grey relational analysis (GRA) to investigate the correlation between parameters and mine water inflow. In this study, we investigated: (1) the detailed statistical characteristics of fault geometry; (2) the degree of fault complexity using E-Ds; and (3) the influence of the water level, water pressure, and structural complexity on water inrush. This allowed us to produce a correlation curve of water pressure, fault complexity, and water inflow.

Geological Conditions

The Zhaizhen coal mine is part of the Xinwen Coalfield, ≈ 9 km northwest of Xintai, Shandong, China (Supplemental Fig. S-1). It has an elevation of 200 ~ 308 m in the north and 200 ~ 170 m in the south. The coal mine is on the axis of the Xinwen syncline; therefore, faults are well-developed. The faults can be divided into three types based on fault throw: small, medium-large, and large fault, which respectively range from 0 to 20 m, 20 to 50 m, and > 50 m. Statistically, there are 23 medium-large faults in this area and lots of secondary faults striking NE, ≈ NS, EW, and especially NEE. Figure 1 shows most of the large-scale faults, of which the fault throw and dip angle are marked by brackets.

The strata in the coalfield are intercalated marine and terrestrial coal-bearing Permo-Carboniferous deposits in

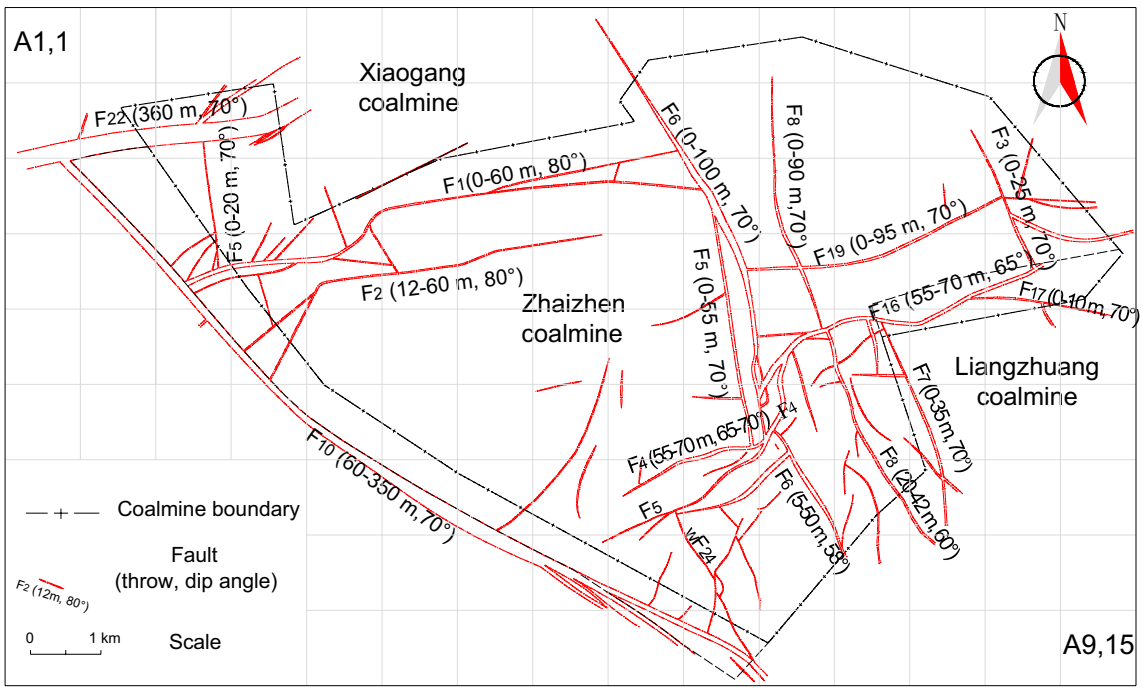

Fig. 1 Tectonic map of the Zhaizhen coal mine

north China. The major aquifers and their characteristics of the study area are listed in Supplemental Table S-1. The limestone aquifers, especially the Ordovician limestone aquifer, are the major cause of mine water inrushes under the present mining conditions. The main coal-bearing strata are the Shanxi and Taiyuan formations including six minable coal seams (numbered 2, 4, 6, 11, 13, and 15). The average thickness of the confined limestone aquifers in coal-measures is less than 10 m, but the Ordovician limestone is about 800 m thick. Therefore, in addition to the high-water pressure, karstification plays an important role in the disasters associated with the Ordovician limestone.

Water-conducting faults or fractures can hydraulically connect aquifers and coal seams. The Ordovician limestone in the study area is a water-abundant aquifer with recharge pathways of meteoric and infiltration water, and the Ordovician limestone itself is very water-rich. However, it has poor recharge in some respects, i.e. a lack of surface outcrops of aquifers and faults. Figure 2 shows the geological profile of the strata including the locations of the coal-bearing strata and confined aquifers. The geological profile shows that the Ordovician limestone is cut by several faults. It is important to understand details about these faults, such as fault throw, dip angle, fault strike length, and cementation, especially for water-conducting faults. In addition, secondary faults associated with the major faults could promote groundwater flow and contribute to rock failure.

Methods

In this study, the degree of fault complexity was described with an *E-Ds* method that combines the fault influence factor (*E*) and fault fractal dimensions (*Ds*), which is built on the fault's characteristics and fractal geometry, respectively. To simplify the calculation, the centre coordinate of each grid was assigned a value for. Then, an appropriate interpolation method was applied to replenish the data when completing the contour maps.

Fault Influence Factor

Previous studies revealed that the major factors controlling fault structure complexity are the fault strike, fault throw, and fault dip angle. Xu et al. (1991) proposed the fault intensity index (*F*) to reflect the degree of structural complexity, which is presented in Eq. (1). It refers to the sum of the product of the fault throw and the horizontal extension of all faults per 10,000 m^2.

$$F = \frac{\sum_{i=1}^{n} l_i h_i}{S}, \tag{1}$$

where l_i is the strike length of the *i*th fault (m); h_i is the throw of the *i*th fault (m); and *S* is the element area (m^2). It has been shown that fault fracture zones greatly damage the integrity of coal measures, and result in more frequent water disasters (Su et al. 2017; Zhou and Li 2001). Therefore, we

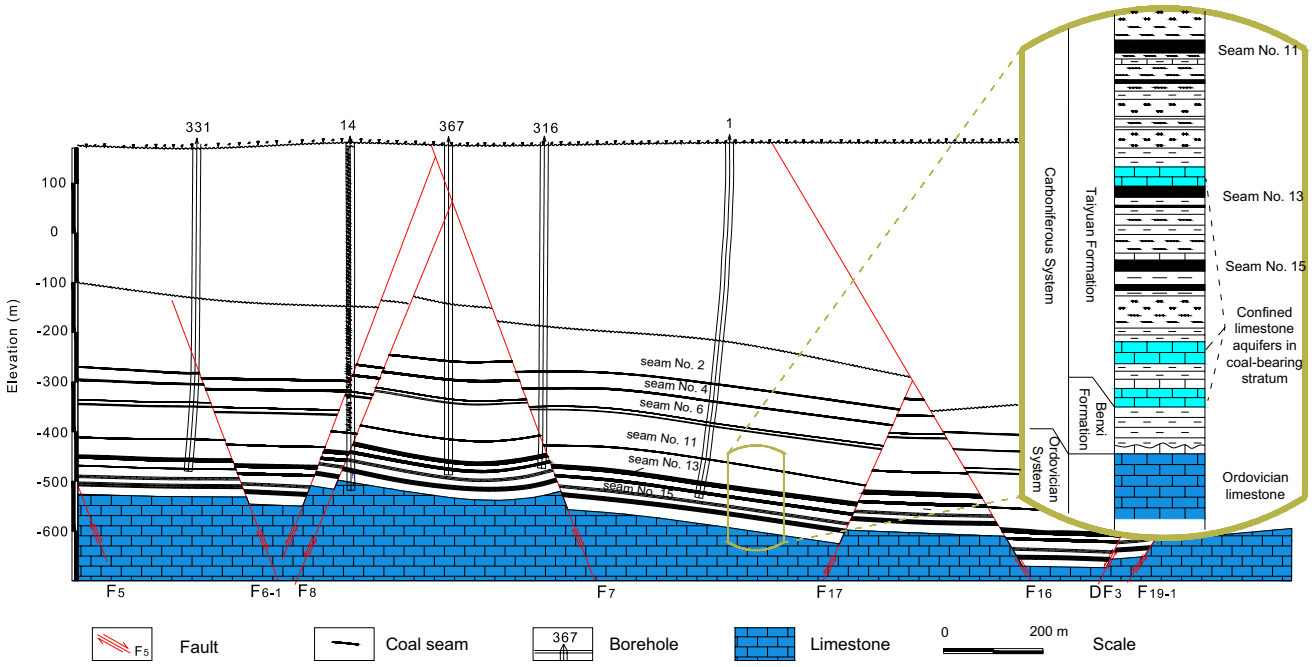

Fig. 2 Geological profile of the Zhaizhen coal mine

used the fault influence factor (*E*), which is developed based on *F*, to present the fault development. It can be expressed as:

$$E = \frac{1}{S}\sum_{i=1}^{n} l_i h_i + M(i = 1, 2, 3 \ldots n), \tag{2}$$

where *M* is the normalized value of the fault intersections and endpoints. Factor *E* reflects the structural characteristics better than the single factor. The details of the method can be presented as follows:

1. Divide the study area into 9 × 15 units with a length of 500 m (Fig. 1).
2. Investigate the fault characteristics statistically and determine the value of *F*
3. Check the fault intersections and endpoints per unit and determine the value of *M*.
4. Determine the value of *E* in per unit and draw a contour map for *E*.

Figure 3 shows one of the grids and Eq. (3) illustrates the calculation. It should be noted that the value of *M* is confirmed after analysis of all units completed because it is related to all fault intersections and endpoints.

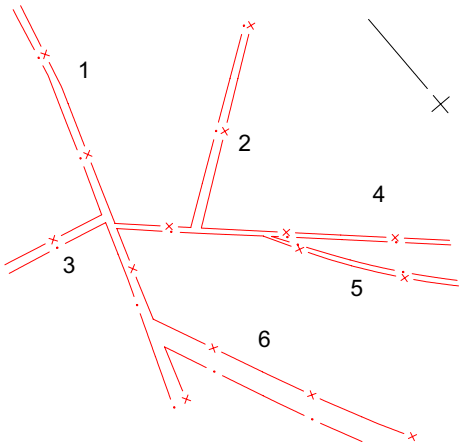

Fig. 3 Fault distribution of unit A 3, 14

$$E = \frac{l_1 h_1 + l_2 h_2 + l_3 h_3 + l_4 h_4 + l_5 h_5 + l_6 h_6}{500 \times 500} + M = 0.364. \tag{3}$$

Fault Fractal Dimension

A fractal dimension is an index for characterizing fractal patterns or sets by quantifying their complexity as a ratio of the change in detail to the change in scale. It has also been characterized as a measure of the space-filling capacity of a pattern that describes how a fractal scale differs from the space it is embedded in (Falconer 2003). Many methods can be used to calculate the fractal dimension, but the self-similarity dimension, *Ds,* is mostly used, which can be expressed as:

$$D_s = dimF(r)\lim_{i\to 0}\frac{\lg N(r)}{-\lg(r)}, \tag{4}$$

where *N(r)* is the number of plans that contain fault traces and *r* is the geometric ratio. Here, we use the box-counting method, which can conveniently be manipulated using a computer, by following these steps:

1. Similar to step one in the calculation of the fault influence factor.
2. Statistically count the number of grids that contain fault traces for different geometric similarity ratios of 1:1, 2:1, 4:1, 8:1, and 16:1 (Fig. 4). A regression line can be obtained by plotting the number *N(r)*, which is at different levels on an lg*N(r)*-lg*(r)* coordinate system. Determine the slopes and their absolute value *Ds* (Supplemental Fig. S-2).
3. Assign the value of *Ds* per unit to the grid center and obtain a contour map of *Ds* by using ArcMap.

A Combined E-Ds Method

Factor *E* involves two fault elements and three parameters (fault throw and strike length; and element area, fault intersections, and endpoints), while the fault fractal dimension is built based on the fault trace. All these factors can influence, to varying degrees, different aspects of a fault's complexity. Therefore, it is necessary to have a

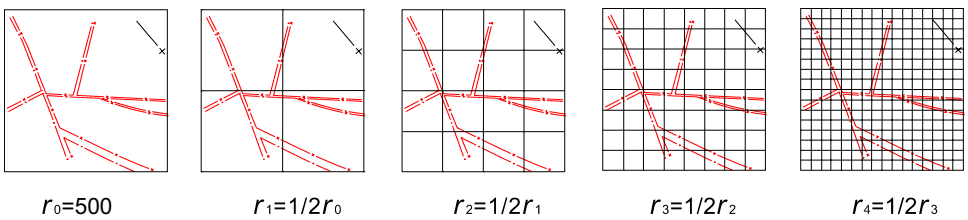

Fig. 4 Grid distribution with different geometric similarity ratios for unit A 4, 13

method that involves all of these factors to reflect the fault complexity more comprehensively. The *E-Ds* method was used to combine the *E* and *Ds*, and then the weight among them was given by the GRA method. The development of medium-large faults is controlled by regional tectonics; therefore, different coalfields in an area have similar fault development. Shi et al. (2015) used water inrush data from three coal mines and proposed a fault control index *I*, which presents the interrelationship between the fault influence factor and fault fractal dimension, as shown in Eq. (5).

$$I = 0.33 \times D_s + 0.67 \times E. \tag{5}$$

The basic steps of GRA are as follows:

(1) Determine the reference sequence and compare the sequence with that of the other parameters.

$$Y = \{Y(k)|k = 1,2,\ldots,n\}, \tag{6}$$

$$X_i = \{X_i(k)|k = 1,2,\ldots,n\} \quad i = 1,2,\ldots,m. \tag{7}$$

(2) Perform nondimensionalization to eliminate the effects of different dimensions.

$$x_i'(k) = x_i(k) / \frac{1}{n}\sum_{k=1}^{n} x_i(k), k = 1,2,\ldots,n; \quad i = 1,2,\ldots,m. \tag{8}$$

(3) Calculate the correlation coefficient.

$$\xi_i(k) = \frac{\min\limits_i \min\limits_k \left|y(k) - x_i(k)\right| + \rho \max\limits_i \max\limits_k \left|y(k) - x_i(k)\right|}{\left|y(k) - x_i(k)\right| + \rho \max\limits_i \max\limits_k \left|y(k) - x_i(k)\right|}. \tag{9}$$

(4) Calculate the correlation degree r_i and weight ω_i of the parameters.

$$r_i = \frac{1}{n}\sum_{k=1}^{n} \xi_i(k), \tag{10}$$

$$\omega_i = r_i / \sum_{k=1}^{n} i_i. \tag{11}$$

The Interpolation Method

The interpolation method is used in dimensional numerical analysis to determine a function from a finite number of values (Berrut 2015). Various interpolation methods (inverse distance weighting, polynomial, spline, and Kriging) are commonly used in different fields (Kouhanestani et al. 2017; Xiao et al. 2016). In addition to these common spatial interpolation methods, there are also methods adapted to rock fractures using fractal interpolation, which is based on the fractal theory's self-affine characteristics (Fu et al. 2017; Xie et al. 2001).

Kriging interpolation is based on geostatistics and is widely used in fields such as geology and meteorology. It is based on local variety theory and the semi-variogram is used as an analysis tool to obtain estimates to ensure a lack of bias and minimal variance. The radial basis function is a real-valued function, where the value is based on the distance from the origin or any other point serving as a center point. Inverse distance weighting interpolation is a simple method, which is based on the similarity principle. The similarity is better if the sample and interpolation are closer to each other and vice versa. The distance between interpolation points and the sample point serves as a weight to determine a weighted average; sample points closer to the interpolation are given more weight. Based on a comparison of these methods and the fault development characteristics, the degree to which damage increases with greater fault density are also considered. Usually, fault development is in a specific direction and fissure development is also controlled by major faults. Therefore, areas further from major faults have correspondingly less likelihood of developing small fissures than areas near the major faults. We used inverse distance weighting interpolation to interpolate the values related to fault complexity.

The inverse distance weighted interpolation method can be expressed as:

$$\hat{Z}(S_0) = \sum_{i=0}^{N} \lambda_i(S_i), \tag{12}$$

where $\hat{Z}(S_0)$ is the predicted value at position S_0; N is the sample quantity acquired around the predicting points in the calculation process; λ_i is the weight of the points, and (S_i) is the measured value of S_i. The weight can be determined by:

$$\lambda_i = d_{i0}^{-p} / \sum_{i=0}^{N} d_{i0}^{-p}, \tag{13}$$

where p is the exponential quantity and d_{i0} is the distance between the predicted point S_0 and the known sample point S_i.

Results

Degree and Classification of Fault Complexity

The *E* and *Ds* values shown in Supplemental Tables S-2 and S-3 were calculated according to the procedures presented

Table 1 Classification of the fault complexity in the Zhaizhen coal mine

Fault complexity degree	*E*	*Ds*
Simple	≤ 0.29	≤ 1.20
Moderate	$0.29 < E \leq 0.46$	$1.20 < Ds \leq 1.38$
Relatively complex	$0.46 < E \leq 0.68$	$1.38 < Ds \leq 1.47$
Complex	> 0.68	> 1.47

above. Based on the regulations for geological coal mine work (State Administration of Work Safety 2014) and field experience, the fault complexity was classified into four degrees, as shown in Table 1.

To understand the fault complexity distribution better, counter maps of *E* and *Ds* (Fig. 5) were drawn based on ArcGIS to present fault complexity, according to the information summarized in Tables S-2 and S-3. The distributions of *E* and *Ds* are similar, illustrating the development of the fault. Comparing the contour distribution in Fig. 5 with that in Fig. 6, it can be seen that factors *E* and *Ds* both influence the complexity classification. Areas E and F were major areas that present the combined effect of *E* and *Ds*. This confirms that both the fault traces on the horizontal section and the scale of the fault influences the fault complexity of a panel.

Table 2 shows the data related to the Ordovician limestone, including the exposed thickness of the limestone (*TL*), groundwater level (*WL*), water pressure (*WP*), fault

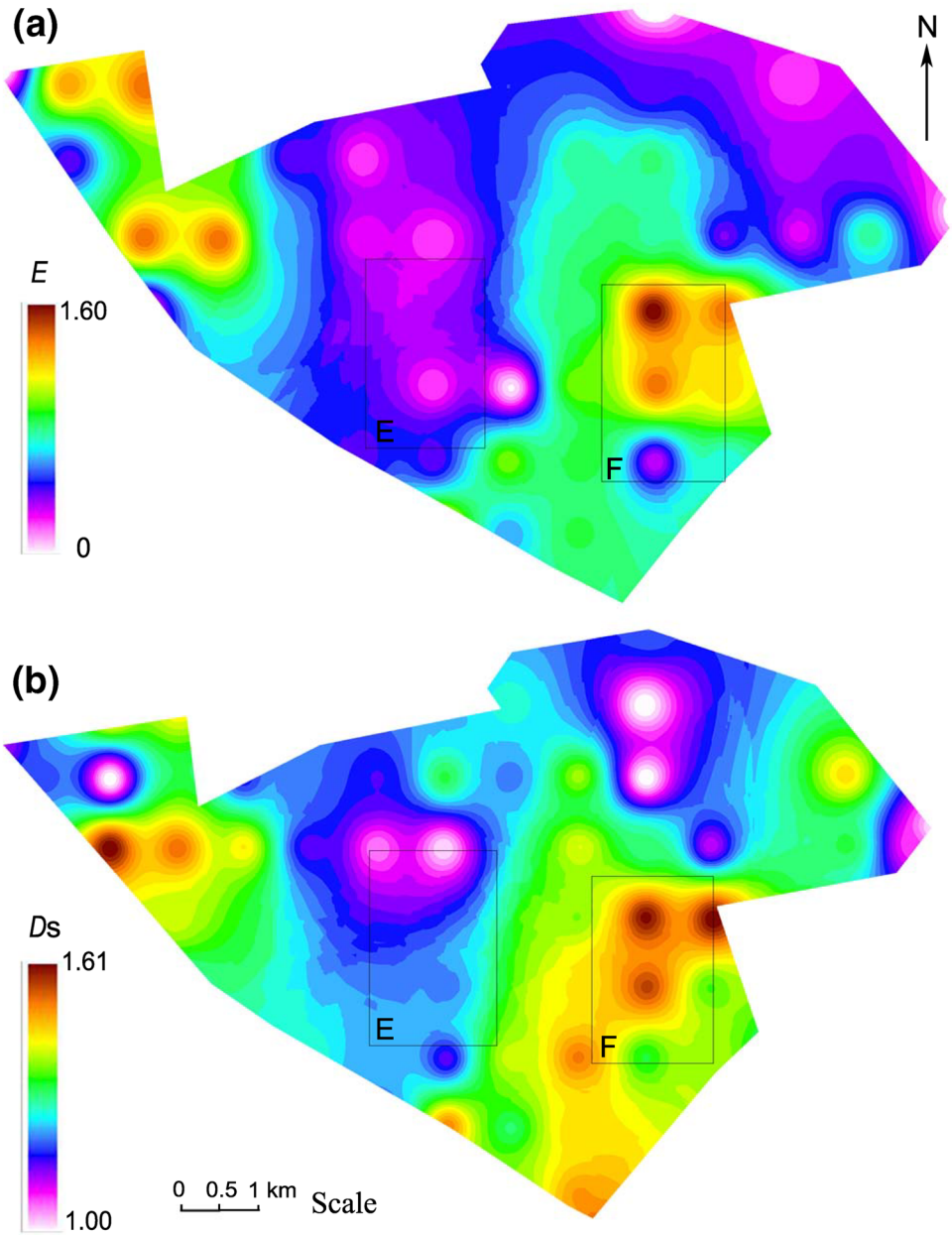

Fig. 5 Contour maps of *E* (**a**) and *Ds* (**b**)

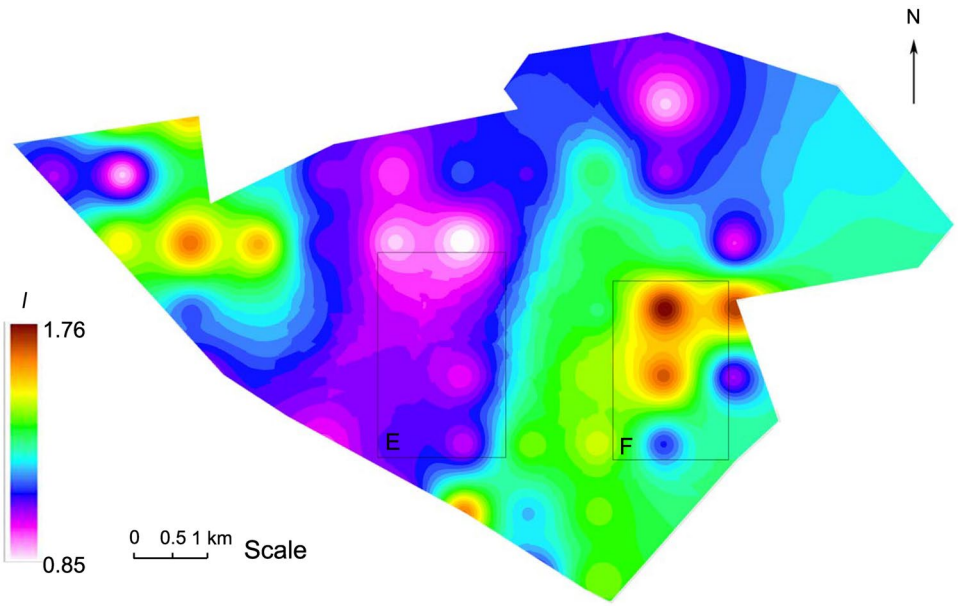

Fig. 6 Contour map of the fault control index *I*

Table 2 Data related to the Ordovician limestone

ID	*TL*/(m)	*WL*/(m)	*WP*/(MPa)	*I*	*WI*/ (m^3/h)
1	95.35	– 206.6	4.9	1.26	51.5
2	125.3	– 206.6	3.9	0.85	13.0
3	114.51	– 313.7	0.8	0.79	2.5
4	96.68	– 250.7	1.5	0.55	8.0
5	68.48	– 213.9	1.5	0.12	3.0
6	90.89	– 151.2	2.4	0.1	1.0
7	107.18	– 160.0	4.5	0.94	25.1
8	76.27	– 178.1	1.8	0.3	1.5
9	125.5	– 211.5	1.2	0.29	1.33
10	69.59	– 137.0	2.5	0.24	0.5
11	72.85	– 139.8	2.6	0.89	1.4
12	92.55	– 108.5	2.8	0.81	0.9
13	47.45	– 188.7	1.8	0.23	6.9
14	63.1	– 199.7	3.1	0.8	2.6
15	57	– 158.9	3.1	0.87	3.1
16	84.4	– 189.6	2.9	0.1	0.83
17	92.3	– 206.6	5.1	1.53	75.5
18	113.2	– 205.9	4.3	1.2	34.2
19	96.5	– 230.1	1.1	0.55	8.0
20	63.1	– 374.7	2.54	0.84	12.2

control index (*I*), and water inflow (*WI*). A distribution map of the mine water inflow corresponding to the geological structure complexity degree was drawn (Fig. 7). Fault complexity is relatively larger in areas where faults are concentrated. The maximum peak had a single borehole water inflow of 80 m^3/h and an *I* value of 1.53, which means that it is a complex fault. Theoretically, water inflow will be greater in a place where faults are concentrated, subject to other factors such as water pressure and aquifuge thickness. Figure 7 clearly shows the corresponding relationship between mine water inflow and fault complexity. Some areas that have more fault complexity will have a corresponding peak.

Correlation Analysis Between Parameters and Mine Water Inflow

Mines, especially in northern China, are now extracting coal from depths exceeding 1000 m. These deep mines in China are mainly threatened by two kinds of water disasters, roof water inrush caused by multi-seam mining and floor Ordovician limestone water inrush (Lan et al. 2016). Of these, the threat from the high-water pressure of floor limestone aquifers is increasingly obvious.

As already mentioned, the limestone aquifer is water-rich due to pervasive fracture systems formed by fissures and cracks. These voids sometimes exhibit a characteristic of high confined pressure but weak water yield, which reveals the importance of the development and connectivity of the fracture system to water abundance (Li et al. 2019). Previous studies have verified that the thickness of the aquifer, fault development and water pressure can all influence aquifer water abundance (Li et al. 2019; Luo and Song 2007; Shi et al. 2019; Zhang 2017). Moreover, the aquifer thickness and structural complexity control the water pressure, which is critical to mine water inrush. Therefore, a systematical and statistical analysis is essential for coal mine safety.

In this case study, the Ordovician limestone aquifer was the major water source of potential mine water inrush. However, the specific thickness of the limestone aquifer was hard to define because the depth of the bottom of the limestone

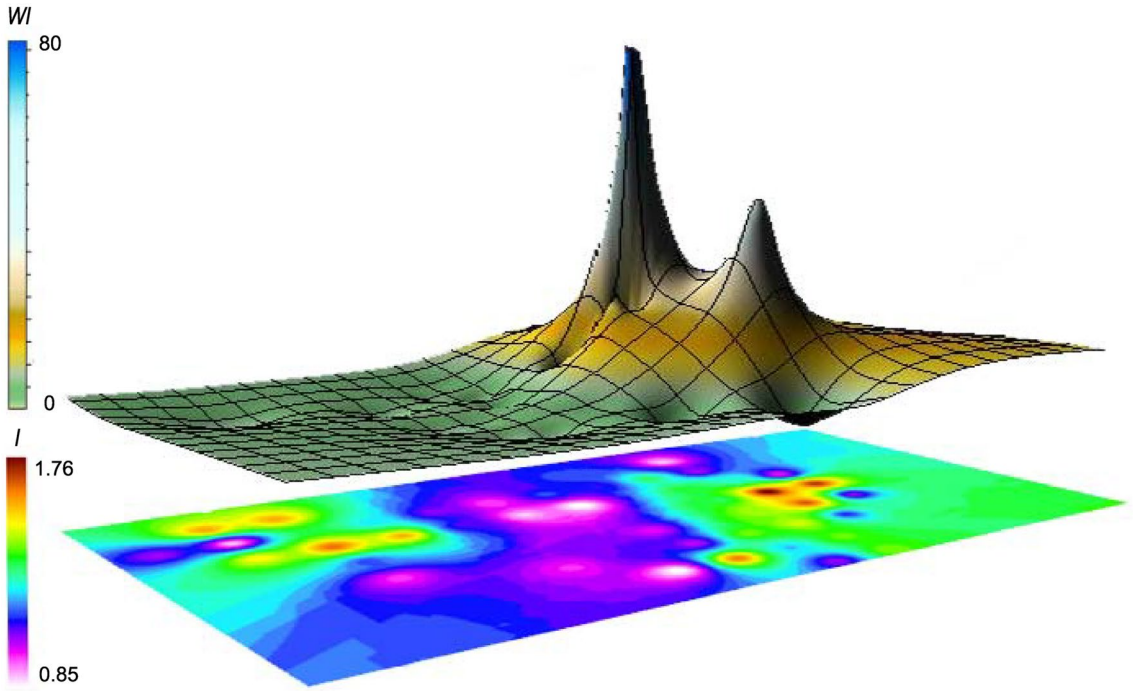

Fig. 7 Distribution of groundwater abundance corresponding to faults complexity degree

strata is unknown. Data listed in Table 2 verify that *WP* and *I* have a nonlinear correlation with *WI*. Based on the aforementioned information, water abundance influences water pressure. Water pressure and fault complexity have a positive nonlinear correlation with water inflow, as shown in Supplemental Figs. S-3 and S-4.

High water pressure, a thick aquifer, and a well-developed fault system will usually lead to a higher water inflow (Gao et al. 2018; Meng et al. 2012; Yin et al. 2017). The fault development, water abundance, water pressure, and mine water inrush form a complex nonlinear system; hence, there could be a nonlinear relationship among them since they are interactional (Shi et al. 2015). GRA is a quantitative description and comparison method with which to examine the development and change of a system. The basic idea is to identify whether the reference data column is closely related to several comparative data columns by determining their geometric similarity, which reflects the degree of correlation between curves. The GRA method can be effective in analyzing nonlinear relationships when the samples have characteristics of less data and large grayscale. The change of water inflow with the other two parameters can be calculated by using Microsoft Excel and GRA (Deng 1989). Based on the calculation steps presented earlier, Eq. (14) expresses the correlation between three parameters and water inflow:

$$Q = 0.24H + 0.24L + 0.26P + 0.26I, \tag{14}$$

where Q is the water inflow, H is the exposed thickness of the Ordovician limestone, P is the water pressure, and L is the groundwater elevation.

Discussion

Mine water inrush accidents are often caused by a geo-structure that transects the aquifers. Statistically, more than 80% of mine water inrush accidents are related to faults (Wu et al. 2008). These faults destroy the continuity and integrity of the rock mass and provide storage space and migration pathways for water. Therefore, investigations of fault development, location, and groundwater content are necessary before mining to effectively prevent coal mine water inrush accidents. The characteristics of faults are critical to water abundance, especially for rock that is otherwise relatively non-porous, such as limestone. Limestone serves as an aquifer mostly because of the cracks, fissures, and karst void space. Many factors can influence the water abundance,

including fault characteristics, aquifer thickness, rock characteristics, folds, and lithological composition. Yin et al. (2017) evaluated sandstone water yield zonation using nine parameters that illustrated the importance of fault development: the sandstone's depth, thickness, and lithological composition; the variation coefficient of the slope of the coal seam; the intensity index of folds in the horizontal direction, and; the length, density, frequency, density, and scale of the fault(s). The major purpose of this paper was to investigate the relationship between fault development and water inflow in certain portions of the Zhaizhen coal mine, where the deeply buried coal seams nos. 13 and 15 are being mined.

The characteristics of faults were fully considered, including the number of faults, fault throw, fault strike length, fault intersections, and fault endpoints. The quantitative relationship between water inflow and the other parameters was analyzed and Eq. (14) was obtained by GRA, based on available quantitative data. A distribution map of water abundance was obtained, which can be a reference for further deep mining research. The Ordovician limestone is the direct source of recharge to groundwater inrush in the Zhaizhen coal mine; therefore, its water abundance is a major concern in groundwater inrush risk assessment. The water-conducting faults and fractures serve as major flow pathways, while the thickness of the aquifer and the groundwater level increase the groundwater pressure and therefore accelerate water flow (Jolley et al. 2007).

As presented, the more faults, the higher the *I* score, usually producing a higher water inflow. The richest groundwater potential zones have been observed to have a high fault density (Yin et al. 2017). To prevent mine water inrush accidents, it is essential to determine the groundwater distribution in aquifers. However, delineating groundwater zonation is a challenging task, which needs considerable surveys, databases, and technical support. Systematically, the investigation of groundwater abundance can be considered from three aspects: geo-structural development, water source, and lithologic features, which correspond to tectonic, hydrogeological, and lithological, respectively. Further development of an evaluation model that considers all the tectonic, hydrogeological and lithological aspects is critical to research on mine water disasters. More accurate geo-structural data requires more borehole data to produce more realistic results to evaluate and predict water abundance and mine water disasters.

Conclusions

The number of faults, fault strike length, fault throw, fault intersections, and endpoints are considered in the *E*-*D*s method, which provides a more reliable evaluation of the degree of fault complexity than the single *E* or *D*s method. Contour maps were drawn by ArcGIS and the distributions of fault complexity are presented for the Zhaizhen coal mine. Also, a distribution map of mine water inflow was drawn based on the results, which can be used as a reference for solving mining problems associated with limestone aquifers. Fault complexity was divided into four qualitative levels: simple, moderate, relatively complex and complex.

The correlation between influential parameters and water inflow showed that there is a nonlinear relationship between water pressure and water inflow, as well as fault complexity and water inflow. A formula was proposed using gray relational analysis that illustrates the correlation between parameters and water inflow.

Supplementary Information The online version contains supplementary material available at https://doi.org/10.1007/s10230-021-00795-x.

Acknowledgements The authors thank the Natural Science Foundation of China (Grant 41472268) for its financial support.

References

Ai T, Zhang R, Zhou HW, Pei JL (2014) Box-counting methods to directly estimate the fractal dimension of a rock surface. Appl Surf Sci 314:610–621. https://doi.org/10.1016/j.apsusc.2014.06.152

Bagde MN, Raina AK, Chakraborty AK, Jethwa JL (2002) Rock mass characterization by fractal dimension. Eng Geol 63(1):141–155. https://doi.org/10.1016/S0013-7952(01)00078-3

Berrut JP (2015) Interpolation. In: Engquist B (Ed), Encyclopedia of Applied and Computational Mathematics. Berlin, pp 710–712

Caine JS, Forster CB (1999) Fault zone architecture and fluid flow: insights from field data and numerical modeling. In: Haneberg W, Mozley P, Moore J, Goodwin L (Eds), Faults and Subsurface Fluid Flow in the Shallow Crust. Geophysical Monograph 113. American Geophysical Union, pp 101–127

Charkaluk E, Bigerelle M, Iost A (1998) Fractals and fracture. Eng Fract Mech 61(1):119–139. https://doi.org/10.1016/S0013-7944(98)00035-6

Deng JL (1989) Introduction to Grey system theory. J Grey Syst 1:103–117

Dimmen V, Rotevatn A, Peacock DP, Nixon CW, Nærland K (2017) Quantifying structural controls on fluid flow: Insights from carbonate-hosted fault damage zones on the Maltese Islands. J Struct Geol 101:43–57. https://doi.org/10.1016/j.jsg.2017.05.012

Eichhubl P, Greene HG, Naehr T, Maher N (2000) Structural control of fluid flow: offshore fluid seepage in the Santa Barbara Basin, California. J Geochem Explor 69:545–549. https://doi.org/10.1016/S0375-6742(00)00107-2

Falconer K (2003) Fractal geometry: mathematical foundations and applications. Wiley, New York

Fang XQ, Fu YJ (2011) Impact of coal mining on karst water systems in north China. Proced Earth Plan Sci 3:293–302. https://doi.org/10.1016/j.proeps.2011.09.097

Fu Y, Zheng ZY, Xiao R, Shi HB (2017) Comparison of two fractal interpolation methods. Phys A 469:563–571. https://doi.org/10.1016/j.physa.2016.11.120

Kouhanestani Z, Dehdar S, Taatpour F (2017) Evaluation of spatial interpolation methods for some groundwater qualitative parameters of Najafabad Plain. Isfahan Model Earth Syst Environ 1:1–8. https://doi.org/10.1007/s40808-017-0355-3

Gartrell A, Zhang YH, Lisk M, Dewhurst D (2004) Fault intersections as critical hydrocarbon leakage zones: integrated field study and numerical modelling of an example from the Timor Sea, Australia. Mar Pet Geol 21:1165–1179. https://doi.org/10.1016/j.marpetgeo.2004.08.001

Gao R, Yan H, Ju F, Mei XC, Wang XL (2018) Influential factors and control of water inrush in a coal seam as the main aquifer. Int J Min Sci Tech 28(2):187–193. https://doi.org/10.1016/j.ijmst.2017.12.017

Jolley SJ, Barr D, Walsh JJ, Knipe RJ (2007) Structurally complex reservoirs: an introduction. Geol Soc Spec Publ 292:1–24. https://doi.org/10.1144/SP292.1

Kang YS, Liu QS, Xi HL, Gong GQ (2018) Improved compound support system for coal mine tunnels in densely faulted zones: a case study of China's Huainan coal field. Eng Geol 240:10–20. https://doi.org/10.1016/j.enggeo.2018.04.006

Lan H, Chen DK, Mao DB (2016) Current status of deep mining and disaster prevention in China. Coal Sci Technol 44(1):39–46 ((**in Chinese**))

Li DR, Yang S (1975) A discussion on the water-rich characteristics and the position in fractured structure zones with different mechanical properties. Chin J Geol 3:220–229 ((**in Chinese**))

Liu HL, Li LC, Li ZC, Yu GF (2017) Numerical modelling of mining-induced inrushes from subjacent water conducting karst collapse columns in northern China. Mine Water Environ. https://doi.org/10.1007/s10230-017-0503-z

Li LC, Yang TH, Liang ZZ, Zhu WC, Tang CN (2011) Numerical investigation of groundwater outbursts near faults in underground coal mines. Int J Coal Geol 85(3):276–328. https://doi.org/10.1016/j.coal.2010.12.006

Li WP, Qiao W, Li XQ, Sun RH (2019) Characteristics of water disaster, evaluation methods and exploration direction for controlling groundwater in deep mining. J China Coal Soc 44(8):2437–2448 ((**in Chinese**))

Liang DX, Jiang ZQ, Guan YZ (2015) Field research: measuring water pressure resistance in a fault-induced fracture zone. Mine Water Environ 34(3):320–328. https://doi.org/10.1007/s10230-014-0323-3

Liu RC, Jiang YJ, Li B, Wang XS (2015) A fractal model for characterizing fluid flow in fractured rock masses based on randomly distributed rock fracture networks. Comput Geotech 65:45–55. https://doi.org/10.1016/j.compgeo.2014.11.004

Luo SH, Song YB (2007) Mine water inrush features and countermeasures for the Wanghe coalmine. J Henan Poly U 06:618–623

Mandelbrot BB, Wheeler JA (1982) The fractal geometry of nature. J R Stat Soc 147(4):468

Meng ZP, Li GQ, Xie XT (2012) A geological assessment method of floor water inrush risk and its application. Eng Geol 143–144:51–60. https://doi.org/10.1016/j.enggeo.2012.06.004

Niwa M, Kurosawa H, Ishimaru T (2011) Spatial distribution and characteristics of fracture zones near a long-lived active fault: a field-based study for understanding changes in underground environment caused by long-term fault activities. Eng Geol 119(1):31–50. https://doi.org/10.1016/j.enggeo.2011.01.011

Shi LQ, Singh RN (2001) Study of mine water inrush from floor strata through faults. Mine Water Environ 20(3):140–147. https://doi.org/10.1007/s10230-001-8095-y

Shi LQ, Teng C, Li CS, Wang DD (2015) Influence of fault quantitative on water inrush at floor limestone in Huaheng coal mine. Safety in Coal Mines 46(9):23–26 ((**in Chinese**))

Shi LQ, Qu XY, Han J, Qiu M, Gao WF, Qin DX, Liu HS (2019) Multi-model fusion for assessing the risk of inrush of limestone karst water through mine floor. J China Coal Soc 44(8):2482–2493 ((**in Chinese**))

State Administration of Work Safety (2014) State Administration of Coal Mine Safety. Coal Mine Geological Work Rules. Beijing: China Coal Industry Publishing House **(in Chinese)**

Su HJ, Jing HW, Zhao HH, Yu LY, Wang YC (2017) Strength degradation and anchoring behavior of rock mass in the fault fracture zone. Environ Earth Sci 76(4):179. https://doi.org/10.1007/s12665-017-6501-4

Wu Q, Wang M, Wu X (2004) Investigations of groundwater bursting into coal mine seam floors from fault zones. Int J Rock Mech Min Sci 41(4):557–571. https://doi.org/10.1016/j.ijrmms.2003.01.004

Wu Q, Zhu B, Li JM, Hong YQ, Qian ZJ (2008) Numerical simulation of lagging water-inrush mechanism of rock roadways near fault zone. J Chin U Min Tech 37(6):780–785 ((**in Chinese**))

Wu Q, Fan ZL, Zhang ZW, Zhou WF (2014) Evaluation and zoning of groundwater hazards in Pingshuo no. 1 underground coal mine, Shanxi Province, China. Hydrogel J 22(7):1693–1705. https://doi.org/10.1007/s10040-014-1138-9

Xie HP, Sun HQ, Ju Y, Feng ZG (2001) Study on generation of rock fracture surfaces by using fractal interpolation. Int J Solids Struct 38(32–33):5765–5787. https://doi.org/10.1016/S0020-7683(00)00390-5

Xiao Y, Gu XM, Yin SY, Shao JL, Cui YL, Zhang QL, Niu Y (2016) Geostatistical interpolation model selection based on ArcGIS and spatio-temporal variability analysis of groundwater level in piedmont plains, northwest China. Springer-plus 5(1):425. https://doi.org/10.1186/s40064-016-2073-0

Xu JP, Liu SD, Wang B, Zhang P, Gui H (2012) Electrical monitoring criterion for water flow in faults activated by mining. Mine Water Environ 31(3):172–178. https://doi.org/10.1007/s10230-012-0184-6

Xu FY, Long RS, Xia YC, Xie SK (1991) Quantitative evaluation and prediction of mine geological structure. J China Coal Soc 4:93–102 ((**in Chinese**))

Yin HY, Shi YL, Niu HG, Xie DL, Wei JC, Lefticariu L, Xu SX (2017) A GIS-based model of potential groundwater yield zonation for a sandstone aquifer in the Juye Coalfield, Shangdong, China. J Hydrol 557:434–447. https://doi.org/10.1016/j.jhydrol.2017.12.043

Zhang R, Jiang ZQ, Zhou HY, Yang CW (2014) Groundwater outbursts from faults above a confined aquifer in the coal mining. Nat Hazards 71(3):1861–1872. https://doi.org/10.1007/s11069-013-0981-7

Zhang YJ (2017) Quantitative evaluation of main control factors of floor water inrush based on multi-information fusion. Coal Min Tech 22(2):87–92 ((**in Chinese**))

Zhou WF, Li GY (2001) Geological barrier-a natural rock stratum for preventing confined karst water from flowing into mines in north China. Environ Geol 40(8):1003–1009. https://doi.org/10.1007/s002540100289